ARTICLES

Supramolecular Aggregation of Regioregular Poly(4-alkyl-2,6-quinoline)s

S. H. Chen,*,† Yan Zhu,‡ Samson A. Jenekhe,‡ A. C. Su,*,§,|| and S. A. Chen||

Department of Materials Science and Engineering, National Dong Hwa University, Hualien 974, Taiwan, Departments of Chemical Engineering and Chemistry, University of Washington, Seattle, Washington 98195-1750, Institute of Materials Science and Engineering and Center for Nanoscience and Nanotechnology, National Sun Yat-sen University, Kaohsiung 804, Taiwan, and Department of Chemical Engineering, National Tsing Hua University, Hsinchu 300, Taiwan

Received: May 20, 2007; In Final Form: August 15, 2007

Phase behavior and morphological features of regioregular, *n*-type semiconducting poly(4-alkyl-2,6-quinoline)s were examined in detail via a combination of thermal, microscopic, and diffraction methods. Two members (P4OQ and P4DQ, with *n*-octyl and *n*-decyl substitutions, respectively) in this series were selected as representatives. Results indicate the dominance of lamellar mesophase throughout the experimentally accessed temperature range (from ambient to above 300 °C), with lamellar spacing well-correlated with side-chain length and temperature. Optical textures observed via polarized light microscopy reveal clear domain-wall features in P4OQ but more solid-like characteristics for P4DQ; improved lamellar order was also observed for P4DQ as compared to P4OQ. These signify stronger tendency toward supramolecular self-assembly with increasing side-chain length. A model of molecular arrangement in the lamellar mesophase in which the free volume is identified as the gap between tips of extended (and interdigitated) side chains and the backbone of the neighboring chain is proposed to account for the observed variation of layer spacing with side-chain length and temperature. The presence of nanodomains (similar to those previously reported for *p*-type conjugated polymers) is also identified in the present *n*-type series, implying general existence of this inherent morphological heterogeneity in semiconducting hairy-rod polymers. This means that molecular aggregation is determined solely by ground-state intermolecular forces; differences in carrier transport characteristics are irrelevant during morphological development. Origins of these nanodomains are discussed in terms of backbone folding (via inherent chemical defects or elastic bending) as well as fringed-micelle aggregates.

Introduction

Supramolecular self-assembly in semiconducting polymers is an important issue in terms of fundamental understanding in the molecular arrangement due to secondary forces in general as well as subsequent effects on optoelectronic properties in particular.[1] Previous observations[2−11] have shown that *p*-type conjugated polymers covalently grafted with alkyl arms such as poly(1,4-phenylenevinylene)s (PPVs),[2−4] poly(3-alkylthiophene)s (PTs),[5,6] and poly(2,7-fluorene)s (PFs)[7−11] are generally mesomorphic in nature. This is interpreted in terms of the tendency toward segregation between the flexible aliphatic arms and the rigid aromatic backbones, i.e., "amphiphilicity" of these hairy-rod polymers with built-in incompatibility between aliphatic and aromatic constituents.[3,4,12,13] For these two series, we have also demonstrated that films cast from dilute solutions are typically composed of weakly coalesced domains ca. 10 nm in size; the origin of the nanodomains is not yet clear but was tentatively attributed to collapsed chains upon solvent removal. It is therefore of interest to see if these features may be generalized to other hairy-rod systems.

Here we report detailed morphological observations on poly(4-alkyl-2,6-quinoline)s (P4AQs, cf. inset of Figure 2a for the general chemical structure) that were recently designed and synthesized to possess high regioregularity and to exhibit *n*-type semiconducting characteristics.[14,15] The backbone of P4AQs comprises quinoline units that bestow high electron affinity (and hence the *n*-type semiconducting characteristics, in contrast to PPVs and PFs) as well as dipolar interbackbone interactions. We show that solution-cast P4AQ films are sanidically mesomorphic throughout the experimentally accessed temperature range (from ambient to above 300 °C), with lamellar spacing well-correlated with the side-chain length. Temperature dependence of the layer spacing reveals thermal expansion coefficients on the order of 400 ppm/K, commensurate with the mesomorphic characteristics. The presence of nanometer-sized domains, similar to those previously reported for *p*-type conjugated polymers, is also identified in this *n*-type case, implying irrelevance of the excited-state characteristics in ground-state molecular aggregation as well as the general existence of morphological heterogeneity in semiconducting polymers.

Experimental Section

Two samples of P4AQs were studied: P4OQ with covalently attached *n*-octyl arms and P4DQ with *n*-decyl arms. Detailed

* To whom correspondence should be addressed.
† National Dong Hwa University.
‡ University of Washington.
§ National Sun Yat-sen University.
|| National Tsing Hua University.

10.1021/jp073893r CCC: $37.00 © 2007 American Chemical Society
Published on Web 10/11/2007

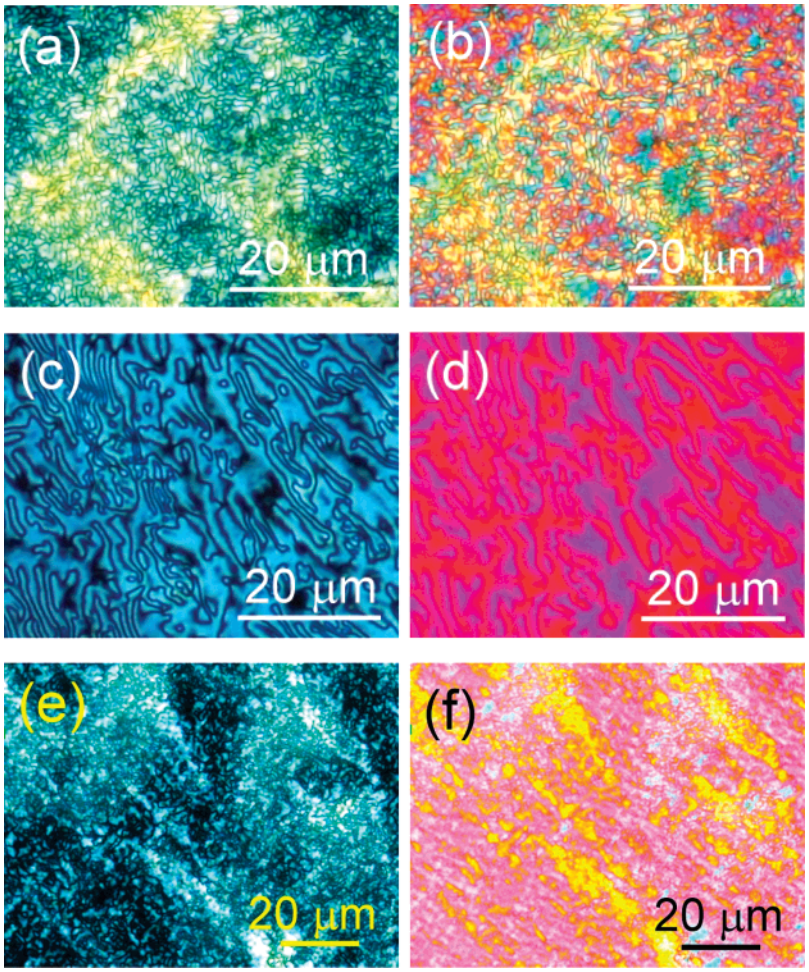

Figure 1. Cross-polarized optical micrographs of P4AQ films (cast from 0.2% toluene solution) after programmed cooling (20 °C/min) from 350 °C (P4OQ) or 300 °C (P4DQ) to room temperature. Thick regions of P4OQ films exhibit (a) fine Schlieren-like features and (b) domain-wall texture upon insertion of the gypsum plate. These liquid-crystalline characteristics are more clearly identifiable in the corresponding micrographs (c and d, respectively) obtained from a thinner region. Micrographs (e) (cross-polarized) and (f) (with gypsum plate inserted) for P4DQ indicate comparatively stronger solid-like characteristics.

procedures in synthesis and characterization have been given previously;[14,15] it suffices to state here that these are of practically perfect head-to-tail regularity, with number-average molecular mass $M_n = 4.3$ and 5.3 kDa for P4OQ and P4DQ, respectively, as determined from end-group analysis via nuclear magnetic resonance spectroscopy; corresponding values of polydispersity index were PDI = 3.5 and 4.0 respectively, as determined via size-exclusion chromatography using polystyrene standards. Instrumental and operational details of optical (PLM), transmission (TEM) and field emission scanning electron microscopic (FESEM) observations as well as X-ray diffraction (XRD) studies are similar to those previously reported.[10,11] Films were drop-cast from dilute toluene solutions (ca. 0.1% for TEM specimens and 0.2% for others) prepared by dissolution in toluene within a hot water bath (kept at ca. 90 °C) and used while still warm.

Results and Discussion

Mesophase Behavior. The mesomorphic nature of regioregular P4AQs is best demonstrated by the cross-polarized optical micrographs of P4OQ film (after thermal cycling at 20 °C/min between room temperature and 350 °C) shown in Figures 1a−1d. Thick regions exhibit fine Schlieren-like features (Figure 1a) and domain-wall texture upon insertion of the gypsum plate (Figure 1b). These liquid-crystalline characteristics are more easily identifiable in the corresponding micrographs (Figures 1c and 1d) obtained from a thinner region. In comparison, optical texture in PLM micrographs of P4DQ films after thermal cycling between room temperature and 300 °C) is more solid-like (Figures 1e and 1f).

TABLE 1: Summary of Layer Spacing Values in Figure 4

temp (°C)	P4OQ layer spacing (nm)	P4DQ layer spacing (nm)	difference (nm)
300	1.744	2.030	0.286
250	1.711	2.004	0.293
200	1.678	1.964	0.286
150	1.644	1.930	0.286
100	1.616	1.888	0.272
30	1.578	1.833	0.255

Given in Figure 2 are representative XRD profiles of P4OQ upon stepwise changes in temperature. There was only limited structural order in the as-cast film (cf. bottom curve in Figure 2a). With increasing temperature, increased mobility allows for structural reorganization (which started at ca. 150 °C) into lamellar order with clear first- and second-order reflections above 200 °C. The lamellar order improves with increasing temperature up to 300 °C as indicated by sharpened reflections (cf. Figure 2b). These reflections correspond to a 1D layered arrangement, as only one lattice parameter can be identified. At the highest temperature reached (350 °C), this lamellar

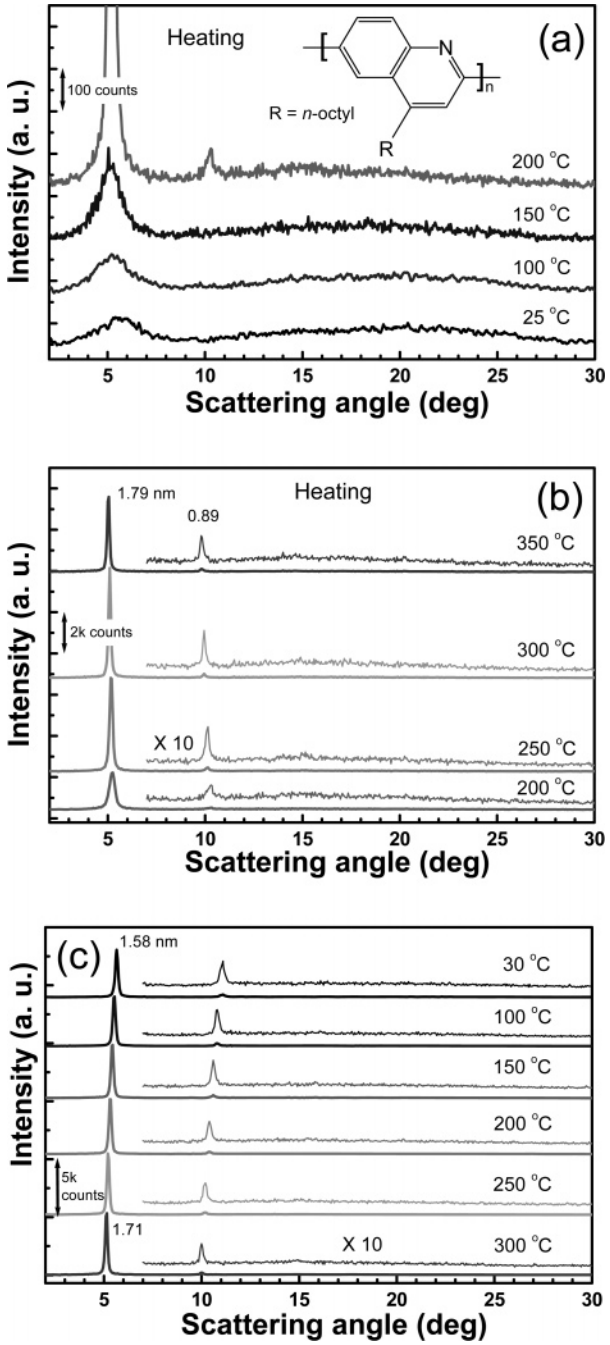

Figure 2. High-temperature XRD profiles of P4OQ upon stepwise changes in temperature: (a,b) the heating sequence toward 350 °C and (c) the subsequent cooling sequence. Thinner lines in (b) and (c) are 10-times magnified in the intensity scale to give finer details.

structure remains stable, although the peak intensities decrease slightly. This implies a thermodynamic transition to a lower order (nematic or isotropic) structure at a higher temperature (which, however, could not be directly identified as interferences from thermal degradation and cross-linking reactions would set in beyond this temperature). The lamellar order remains unaltered in the subsequent cooling from 350 °C (cf. Figure 2c), without signs of transformation into further ordered structure such as a crystalline phase.

Given in Figure 3 are corresponding XRD profiles for P4DQ film, which are basically similar to the case of its shorter side-chain analogue, P4OQ. Qualitative similarities include (1) poorly developed order in the as-cast film, (2) structural reorganization upon heating beyond 150 °C, and (3) retained lamellar order

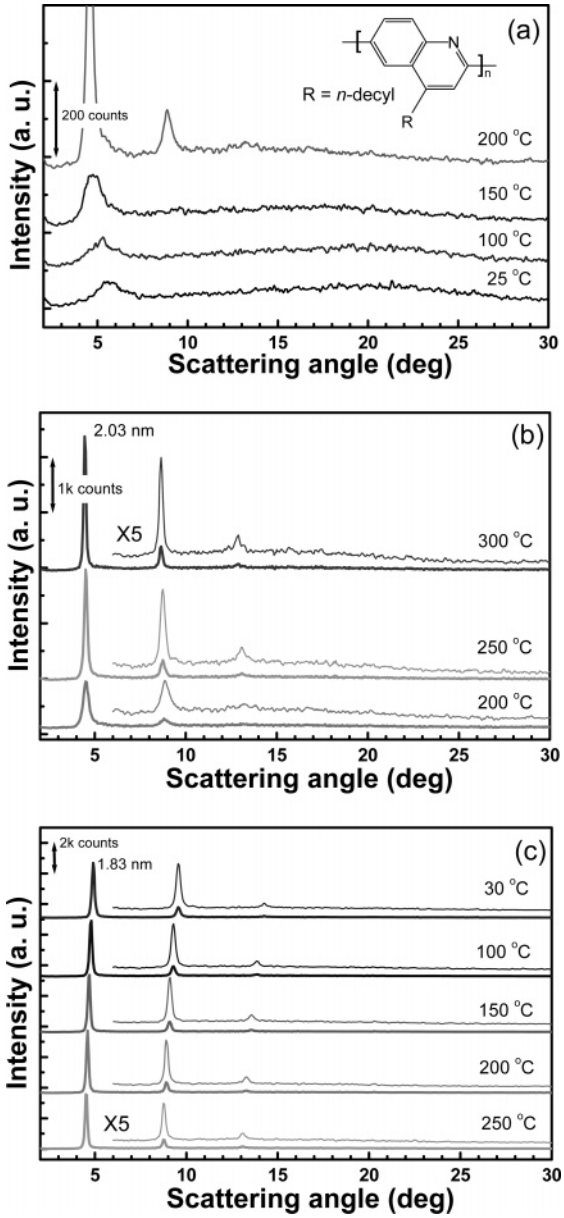

Figure 3. High-temperature XRD profiles of P4DQ upon stepwise changes in temperature: (a,b) the heating sequence toward 300 °C and (c) the subsequent cooling sequence. Thinner lines in (b) and (c) are 5-times magnified in the intensity scale to give finer details.

without discernible crystallization during cooling. There is an important difference though: the longer side chains in P4DQ clearly result in better developed lamellar order, exhibiting the third-order reflection. This agrees with the observed difference in optical texture in Figure 1 and is consistent with the contention that supramolecular self-assembly in these hairy-rod polymers originated from incompatibility between aliphatic side chains and aromatic backbones.[3,4,12,13]

Molecular Packing. More quantitatively, as demonstrated in Figure 4 and summarized in Table 1, the layer spacing exhibits nearly the same temperature dependence, with a nearly constant difference of 0.29 nm (or ca. 0.145 nm/side-chain carbon) at elevated temperatures for P4OQ and P4DQ. This is clearly contradictory to the known 0.125 nm/carbon for the stretched alkyl chain, which we will address in later paragraphs. The corresponding difference at room temperature, however, is 0.255 nm (or 0.128 nm/side-chain carbon) that compares favorably to the expected increment of 0.125 nm/carbon atom if grafted alkyl side chains are stretched transversely to the

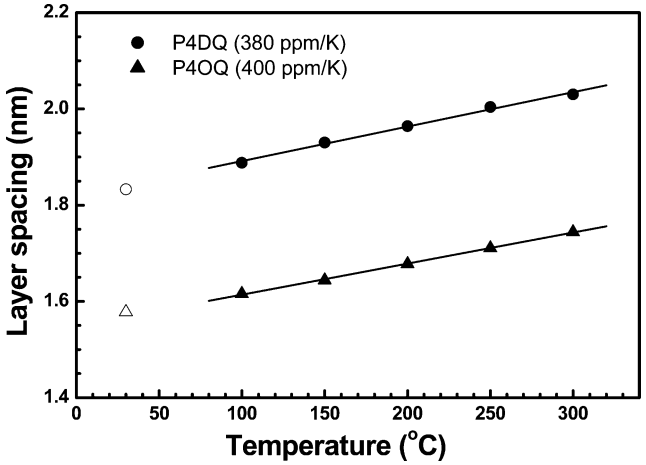

Figure 4. Temperature dependence of layer spacing in the cooling sequence, yielding linear thermal expansion coefficients of 400 and 380 ppm/K for P4OQ and P4DQ, respectively.

backbone axis. This is in accordance with a model of molecular packing conjectured on a previous occasion (cf. Figure 1 in ref 10), where grafted alkyl side chains are extended transversely and fully interdigitated with alkyl arms stretched from the neighboring backbone.

Nevertheless, detailed calculations indicated that free ends of side chains must be kept from neighboring backbones by 0.12 nm to satisfy the observed room-temperature layer spacing values of P4OQ and P4DQ, as schematically demonstrated in Figure 5a. The gap between side-chain tips and the neighboring backbone corresponds to part of the free volume within the supramolecular assembly. This gap of free volume must further increase with increasing alkyl side chain length for an apparent increment of 0.145 nm/side-chain carbon. This may be understood by consideration of increased side-chain motion with increasing carbon number (and degree of rotational freedom of C−C linkages) upon thermal excitation, reminiscent of volume dilation of vibrating sands. In other words, one may envision (cf. Figure 5b) that an increase in temperature results in increased entropy from side-chain motions, which requires that the side chains be more shallowly interdigitated.

The discussion above is based on XRD results of films slowly cooled from above 300 °C, which presumably correspond to the thermally equilibrated mesomorphic structure. In the case of as-cast films, the apparent contribution of 0.10 nm/side-chain carbon on the layer spacing has been previously reported,[14] which corresponds to a slightly modified model in which side chains are tilted from the backbone axis (cf. Figure 4 in ref 11). This as-cast structure, however, is intrinsically metastable, as also demonstrated here in Figures 2 and 3. It is therefore clear that the molecular packing varies strongly with processing condition, consistent with the mesomorphic nature observed here for P4AQs and elsewhere for hairy-rod polymers in general.[1−13]

The proposed model of molecular packing in Figure 5 is also supported by our TEM observations on quenched P4OQ and P4DQ specimens subsequent to shear orientation (at 260 or 270 °C) and thermal annealing for structural perfection at 200 °C. Figure 6 gives representative bright field images (BFI) and the corresponding selected area electron diffraction (SAED) patterns. The SAED patterns generally indicate layered structure in both specimens, which is nevertheless better ordered in the case of P4DQ as similarly observed from XRD results. More interestingly, we note that the layer spacing values (1.65 nm for P4OQ and 1.96 nm for P4DQ, as read from equatorial reflections) are in better accord with those determined via XRD at 200 °C rather than the equilibrated room-temperature values, indicating retained high-temperature molecular arrangement upon quenching. This is consistent with the notion that the supramolecular assembly is mesomorphic rather than strictly 3D crystalline in its classical sense.

Meridional reflections are observed only for the case of P4DQ, consistent with the better developed and more solid-like structural features. These indicate a monomer repeat length of 0.60 nm, which is slightly shorter than that (0.63 nm) obtained from molecular simulation by assuming perfect coplanarity of the P4AQ backbone. We take this as a hint for fluctuated ring torsions (by 18° in average) from the idealized all trans conformation depicted in Figure 5.

Nanodomains. More interestingly, closer examination of BFI in Figure 6 indicated the general presence of heterogeneities

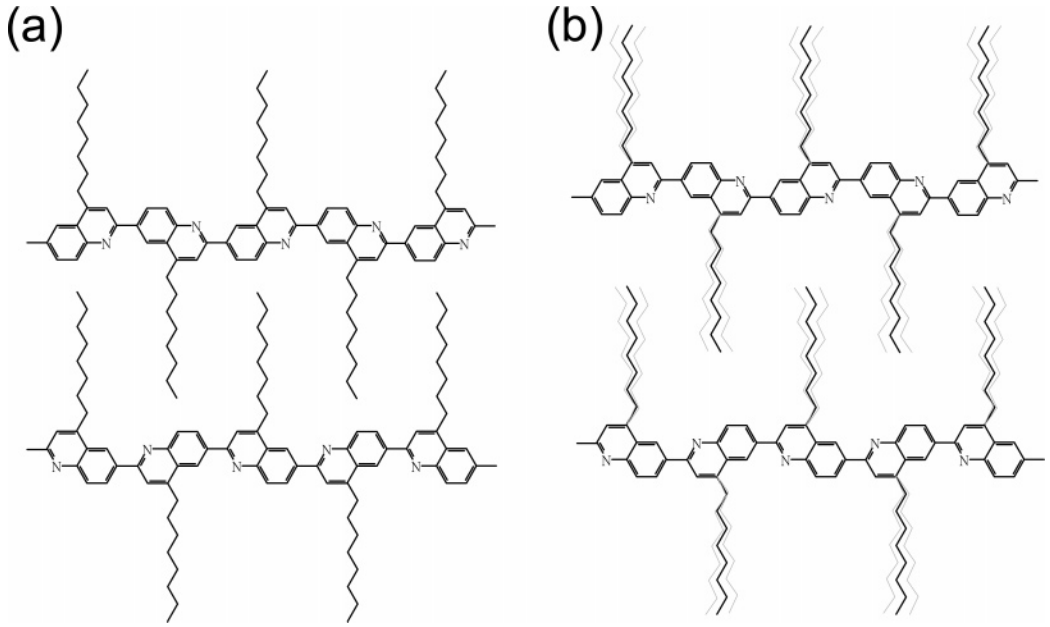

Figure 5. Schematic representation of supramolecular self-assembly in P4AQs: (a) at low temperatures and (b) at elevated temperatures. Note that an increase in temperature favors the high-entropy case of increased side-chain motion, which results in shallower interdigitation of side chains and increased free volume.

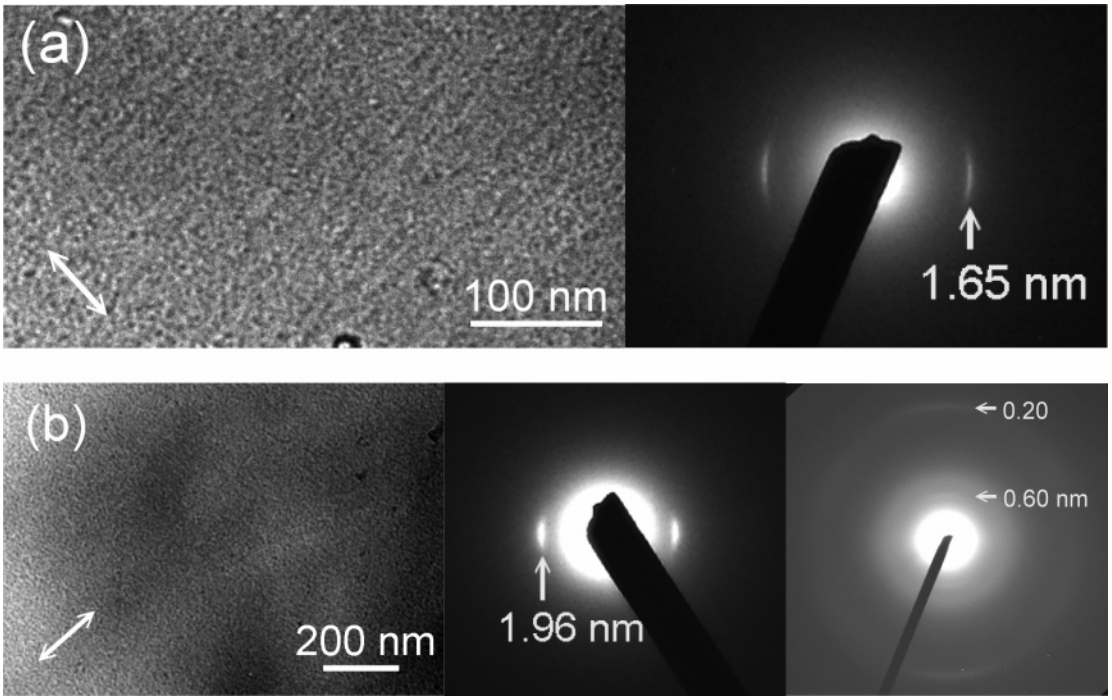

Figure 6. Bright field images (BFI) and the corresponding SAED patterns for oriented specimens of (a) P4OQ (manually sheared at 270 °C, followed by 10 min annealing at 200 °C and quenching in ice water) and (b) P4DQ (manually sheared at 260 °C, followed by 10 min annealing at 200 °C and quenching in ice water). The direction of shear is indicated as two-way arrows in BFI but set to lie along the meridian in the corresponding SAED patterns.

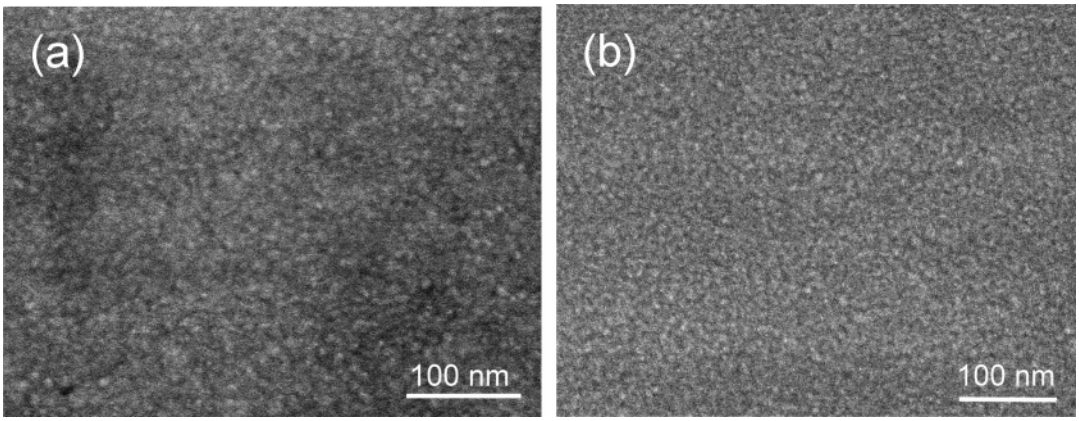

Figure 7. Secondary electron images (SEI) of (a) P4OQ and (b) P4DQ films (both annealed at 200 °C for 10 min before quenching in ice water), showing nanodomains ca. 5−10 nm in size.

approximately 5−10 nm in size. As shown in Figure 7, these features are more easily identified in the secondary electron images (SEI) obtained via FESEM examination of P4OQ and P4DQ films. Similar nanodomain features have been previously reported[2−4,9−11] for *p*-type semiconducting polymers such as PPVs and PFs. It appears that the formation of nanodomains is likely a general feature of hairy-rod polymers, irrespective of their electronic properties. As for the significance of this inherent heterogeneity in the nanometer scale, limited experimental evidence[16,17] has indicated that the size and the orientation of nanodomains may be controlled by proper choice of processing conditions (such as the presence of an electrical field during film formation) and may significantly affect carrier transport behavior of semiconducting polymer films.

Molecular origin of these nanoscale heterogeneities, however, deserves some discussion. On the basis of morphological observations of collapsed single molecules of a PPV derivative,[18,19] we have previously[2−4,9−11] attributed the nanodomains to clusters of collapsed (and loosely folded) chains upon solvent removal during film formation. In the particular case of PPV derivatives, tetrahedral defects[20] have been known to exist, whose presence renders the formation of loose fold feasible. However, subsequent studies on PFs also indicated the existence of nanodomains, for which no counterparts for the tetrahedral defects in PPVs are known. The same difficulty applies also to the present case of P4AQs. Nevertheless, recent atomic force microscopic results[21] indicated folding of alkyl-grafted poly(*p*-phenylene-ethynelene) chains (strictly colinear in terms of chemical structure) on a highly oriented pyrolytic graphite surface, implying that intermolecular attractions are adequate to elastically bend the rigid backbone at least in this 2D case. An alternative interpretation could be that these nanoscale heterogeneities correspond to molecular aggregates that are limited in size due to retarded growth (attributable to interminglement of alkyl side chains)[22] and high rate of nucleation (in view of the inherent incompatibility between aliphatic side chains and aromatic backbones), reminiscent of the classical fringed-micelle picture of polymer crystallites. This interpreta-

tion, however, awaits future studies for confirmation or further modifications.

As a final remark, we would like to point out that although the present P4AQs are considered *n*-type semiconducting in view of the higher electron affinity (and hence the lowered electron injection barrier and increased hole-blocking characteristics), the electron mobility in the film state is not necessarily high (in fact, less than impressive as indicated by preliminary results obtained from field-effect measurements). This is quite understandable as carrier mobility is strongly affected by structural/constitutional defects[23,24] as well as morphological inhomogeneities[16,17,25] that serve as traps or blocking barriers for charge carriers. The issue, however, is beyond the present scope and will be addressed in future occasions.

Conclusion

Phase behavior and morphological features of regioregular, *n*-type semiconducting poly(4-alkyl-2,6-quinoline)s were examined via a combination of microscopic and diffraction methods. Results indicate the dominance of sanidic mesophase throughout the experimentally accessed temperature range (from ambient to 350 °C), with lamellar spacing well-correlated with the side-chain length. Temperature dependence of the layer spacing reveals thermal expansion coefficients on the order of 400 ppm/K, commensurate with the suggested mesomorphic nature. A modified model of molecular packing in which thermally activated "shaking" (induced by rotational degree of freedom of C−C linkages) of interdigitated (and hence "confined") side chains is allowed; this accounts for diffraction results obtained for the present P4AQ series in a wide range of temperatures. The presence of nanodomains (ca. 5−10 nm in scale), similar to those previously reported for *p*-type conjugated polymers, is also identified in this *n*-type case, implying the general existence of such inherent morphological heterogeneity in semiconducting hairy-rod polymers.

Acknowledgment. Financial support from the National Science Council (Grant Nos. NSC 95-2752-E-007-007-PAE and 95-2221-E-007-267) is gratefully acknowledged. Work at the University of Washington was supported by the NSF (CTS-0437912) and NSF STC MDITR (DMR-0120967).

References and Notes

(1) Chen, S. H.; Su, A. C.; Huang, Y. F.; Su, C. H.; Peng, G. Y.; Chen, S. A. *Macromolecules* **2002**, *35*, 4229.

(2) Chen, S. H.; Su, A. C.; Chou, H. L.; Peng, K. Y.; Chen, S. A. *Macromolecules* **2004**, *37*, 167.

(3) Chen, S. H.; Su, A. C.; Han, S. R.; Chen, S. A.; Lee, Y. Z. *Macromolecules* **2004**, *37*, 181.

(4) Chen, S. H.; Su, C. H.; Su, A. C.; Chen, S. A. *J. Phys. Chem. B* **2004**, *108*, 8855.

(5) Kim, D. H.; Park, Y. D.; Jang, Y.; Yang, H.; Kim, Y. H.; Han, J. I.; Moon, D. G.; Park, S.; Chang, T.; Chang, C.; Joo, M.; Ryu, C. Y.; Cho, K. *Adv. Funct. Mater.* **2005**, *15*, 77.

(6) Kline, R. J.; McGehee, M. D.; Kadnikova, E. N.; Liu, J.; Fréchet, J. M. J.; Toney, M. F. *Macromolecules* **2005**, *38*, 3312.

(7) Teetsov, J. A.; Vanden, Bout, D. A. *J. Am. Chem. Soc.* **2001**, *123*, 3605.

(8) Teetsov, J.; Vanden Bout, D. A. *Langmuir* **2002**, *18*, 897.

(9) Chen, S. H.; Chou, H. L.; Su, A. C.; Chen, S. A. *Macromolecules* **2004**, *37*, 6833.

(10) Chen, S. H.; Su, A. C.; Su, C. H.; Chen, S. A. *Macromolecules* **2005**, *38*, 379.

(11) Chen, S. H.; Su, A. C.; Chen, S. A. *J. Phys. Chem. B* **2005**, *109*, 10067.

(12) Watanabe, J.; Harkness, B. R.; Sone, M.; Ichimura, H. *Macromolecules* **1994**, *27*, 507.

(13) Ou-Yang, W. C.; Chang, C. S.; Chen, H. L.; Tsao, C. S.; Peng, K. Y.; Chen, S. A.; Han, C. C. *Phys. Rev. E* **2005**, *72*, 031802.

(14) Zhu, Y.; Alam, M. M.; Jenekhe, S. A. *Macromolecules* **2002**, *35*, 9844.

(15) Zhu, Y.; Alam, M. M.; Jenekhe, S. A. *Macromolecules* **2003**, *36*, 8958.

(16) Jeng, U.; Hsu, C. H.; Sheu, H. S.; Lee, H. Y.; Inigo, A. R.; Chiu, H. C.; Fann, W. S.; Chen, S. H.; Su, A. C.; Lin, T. L.; Peng, K. Y.; Chen, S. A. *Macromolecules* **2005**, *38*, 6566.

(17) Inigo, A. R.; Chang, C. C.; Fann, W.; White, J. D.; Huang, Y. S.; Jeng, U. S.; Sheu, H. S.; Peng, K. Y.; Chen, S. A. *Adv. Mater.* **2005**, *17*, 1835.

(18) Hu, D.; Yu, J.; Wong, K.; Bagchi, B.; Rossky, P. J.; Barbara, P. F. *Nature (London)* **2000**, *405*, 1030.

(19) Mehta, A.; Kumar, P.; Dadmum, M. D.; Zheng, J.; Dickson, R. M.; Thundat, T.; Sumpter, B. G.; Barnes, M. D. *Nano Lett.* **2003**, *3*, 603.

(20) Padmanaban, G.; Ramakrishnan, S. *J. Am. Chem. Soc.* **2000**, *122*, 2244.

(21) Lei, S. B.; Deng, K.; Yang, Y. L.; Qing-Dao Zeng, Q. D.; Wang, C.; Ma, Z.; Wang, P.; Zhou, Y.; Fan, Q. L.; Huang, W. *Macromolecules* **2007**, *40*, 4552.

(22) Chen, S. A.; Chang, E. C. *Macromolecules* **1998**, *31*, 4899.

(23) Tseng, H. E.; Peng, K. Y.; Chen, S. A. *Appl. Phys. Lett.* **2003**, *82*, 4086.

(24) Tseng, H. E.; Liu, C. Y.; Chen, S. A. *Appl. Phys. Lett.* **2006**, *89*, 233510.

(25) Tseng, H. E.; Liu, C. Y.; Chen, S. A. *Appl. Phys. Lett.* **2006**, *88*, 042112.